Nine-phase Permanent Magnet Motor Drive System for Ultra High-speed Elevator

Eunsoo Jung[1], Hyunjae Yoo[1], Seung-Ki Sul[1], Hong-Soon Choi[2], and Yun-Young Choi[3]

[1)] School of Electrical Engineering & Computer Science, Seoul National University, Seoul, 151-744, Korea

[2)] School of Electrical Engineering, Kyungpook National University, Sangju, Gyeongbuk, 742-711, Korea

[3)] Hyundai Elevator Co., Ltd., Icheon, Gyeonggi, 467-734, Korea

***Abstract* − In this paper, a 9-phase Permanent Magnet (PM) synchronous motor drive system based on multiple 3-phase conventional drive systems has been proposed. A 9-phase motor has been developed as a traction motor for a world record ultra high speed elevator. The simplified mathematical model, which can be incorporated with 3-phase current controller, has been derived. The feasibility and the validity of the proposed drive system have been demonstrated by experimental results of the scaled version of a prototype 9-phase motor.**

***Index Terms* − multiphase motor, ultra high-speed elevator, AC motor drives**

I. INTRODUCTION

Recently, with advances in building technology and materials, high-rise buildings are getting more popular. Especially, the number of ultra high-rise building that is taller than ever is getting increased. The advent of modern high-rise buildings has brought about the need for high-speed lift systems to provide quick access with high reliability [6]. Moreover, an elaborate control technique is also needed to give a comfort to passengers.

The Voltage Source Inverter (VSI) fed Permanent Magnet (PM) motor is widely used in elevator applications due to its high efficiency, compact size and fine control performance. However, high power elevator systems such as an ultra high-speed elevator and a double deck elevator demand a peak power rating more than 1 MW. Three-phase system, therefore, may not be suitable due to the current limitation of power devices.

In high power drive systems, the multiphase motors can be attractive solution over the size limitation of individual inverters. Furthermore, the multiphase motors have several advantages such as a low torque ripple, a fault-tolerance capability, and a reduction in the per phase power rating [1]-[3].These advantages lead a dual stator PM motor to be adopted in the state-of-the-art elevator [4]. In [4], each set of windings are separately connected to the own 3-phase inverter which employs six IGBT modules connected in parallel because of per phase ratings of the inverter. The power devices that are derated have been used because of the parallel connection of the IGBTs. A control method under open fault condition using other five phase has been proposed to minimize the total power derating of the system in [2], [3]. However, when a short fault or a DC-link side fault occur, a relevant inverter should be detached from the system and the total power rating of the system is reduced to the half of the normal operating condition.

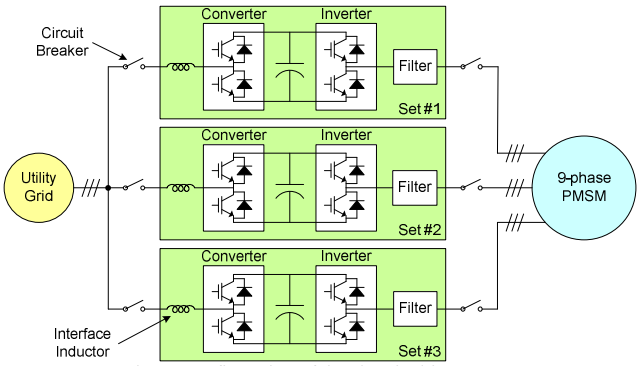

Fig. 1. Configuration of the electric drive system

In this paper, a 9-phase PM motor driven by triple VSIs has been proposed as shown in Fig 1. The mathematical modeling of the proposed 9-phase motor has been derived and it has been divided to three independent 3-phase motor models. By using this simplified model, three conventional synchronous frame Proportional and Integral (PI) controllers can be easily applied. Moreover, due to the symmetry of the three 3-phase motor models and controllers, the ripple component in the total torque can be reduced conspicuously. Experiments with the 15kW 9-phase prototype motor, which is a scaled version of the traction machine of the ultra high-speed elevator, have been performed to evaluate the validity of the proposed drive system.

II. ELECTRIC DRIVE SYSTEM DESIGN

The electrical drive system for the elevator is shown in Fig. 1 which consists of a 9-phase PM motor, three PWM inverters, PWM converters and other components.

A. Traction Machine – 9-phase PM Motor

A computer simulation based on a simple mechanical model has been performed to calculate the desired capacity of the traction machine. Table I shows the specification of the elevator system. The rated speed upward is 1,080 m/min and the rated capacity for passengers is 1600 kg. The total mass to calculate the inertia in the simulation has been assumed as 40,000 kg considering the weight of the mechanical system such as a cage, counterweight, a main rope and a compensation rope.

TABLE I
SPECIFICATION OF THE ULTRA HIGH-SPEED ELEVATOR

Rated Capacity	1600 kg
Rated Speed	Up 1,080 m/min Down 600 m/min
Travel Height	Up to 540 m

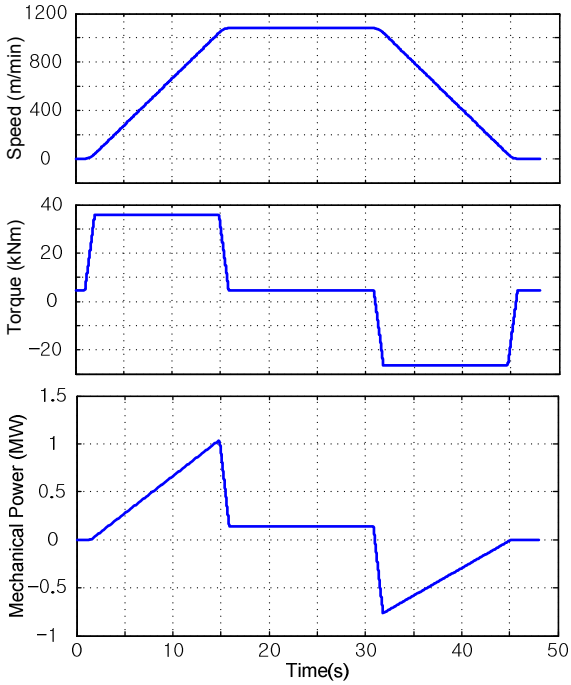

Fig. 2. Simulation result for the elevator operation. (Top: Speed reference of the elevator car, center: Torque to accelerate the elevator car, bottom: Mechanical output power of the traction machine).

The simulation result is shown in Fig. 2. The top figure shows the speed reference profile. The acceleration value is 1.3 m/s^2. This is the maximum (critical) value which passengers do not feel uncomfortable. The necessary torque is 36 kNm at this time. According to the simulation results, the traction machine requires 1 MW maximum mechanical power to meet the specification in table I. These results are based on an ideal condition. Reflecting the loss of the motor, total power rating should be increased further.

Assuming that the total efficiency of the whole mechanical system including some margin is 0.8, the maximum output power of the motor should be 1.25 MW. However, because medium voltages are generally not available for the commercial buildings where the elevators are installed, it is difficult to implement such high power system with the low utility voltage, usually 380 V or 440V. To yield such high power in the low voltage, a three phase motor of which rated current is more than 3,000 A is necessary. This current rating is too large to implement one three-leg VSI using a commercial 1200 V IGBTs' current rating device.

To reduce the current rating of each phase, a nine-phase PM motor has been proposed for the ultra high-speed elevator. In addition, the multiphase motor is possible to improve the ride comfort and safety of the passengers, due to lower torque ripples and higher reliability in the system level.

B. Motor Drive system – PWM Inverters and Converters

The elevator driven by an electrical motor demands a broad dynamic power range to deal with the motoring and generating power which regularly occur during the acceleration and the deceleration operation. A voltage source PWM inverter-converter set is commonly used to manage the power flow between the mechanical system and the electric utility. By the PWM converters, it is possible that the power factor at the utility side is maintained as unity. In addition, energy loss caused by the dynamic braking resistor can be saved because the PWM converter has inherent regenerating capability as well as rectifying capability [6].

To drive a high power 9-phase PM motor, three 3-leg VSIs are used at the motor side and other three VSIs are used at the utility side as shown in Fig. 1. Three DC-links are separated from each other because a common DC-link structure is not capable of supporting severe faults in the DC-bus [4]. Each inverter-converter set operates independently and consists of six IGBTs of which rating is 1200 V, 1200 A at 80ºC. The rated power of each inverter-converter set is 450 kW and thus the overall system can deliver 1.35 MW of power.

The PWM converters include interface inductors to regulate the current to the utility side. The size of these interface inductors is determined by the magnitude of the switching ripple current. To reduce the switching ripple current to the utility side, carriers of three PWM converters are interleaved with each other by 120º electrical angle difference. As the results, the size of the interface inductor can be reduced significantly.

C. Other Components

There are circuit breakers for the input terminals of the converters and the output terminals of the inverters to increase the reliability of the system. When a fault occurs, the circuit breakers of the corresponding set are opened and then the faulty set can be separated from the whole system. And then remaining sets are still able to perform normal operations. In the case of the separation of one set, the total power rating could be 77% of the rated power of the system.

To increase the reliability of the system, a filter inductor and an RC network are added between the inverter and the motor. The filter inductor and the RC network suppress the spike voltages at the motor terminals and prevent the motor from insulation failure.

III. MODELING AND CONTROL OF THE 9-PHASE PM MOTOR

To operate the proposed drive system, the mathematical model of the 9-phase PM motor should be derived preliminary. And then a control strategy for the system is proposed.

A. The 9-phase PM motor model

The simplified stator winding structure of the proposed motor is shown in Fig. 3. The motor consists of 9 phases and each phase is separated from the next one by 40º electrical angle. Three stator windings which are separated by 120º with each other constitute one three-phase connection. Thus, the motor has triple three-phase stator windings that are all Y-connected. The neutral points of each three-phase set are electrically isolated.

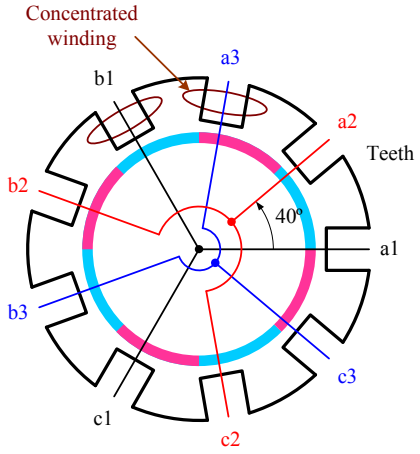

Fig. 3. Simplified winding structure of the proposed motor.

The notations in Fig. 3 represent the phase numbers and the set numbers. For example, the *b2* stands for the *b-phase* of the *second three-phase set*. Because of the inherent winding structure of the proposed surface mounted PM motor shown in Fig. 3(a), the mutual inductance between each two phase winding is independent with the angular displacement [5]. The voltage equation of the *a-phase* of *set 1*, therefore, can be expressed as (1).

$$v_{a1} = R_s i_{a1} + L_{self}\frac{di_{a1}}{dt} + L_m \frac{d}{dt}\left(i_{b1}+i_{c1}+i_{a2}+i_{b2}+i_{c2}+i_{a3}+i_{b3}+i_{c3}\right)+e_{a1} \quad (1)$$

where R_s represents the resistance of the $a1$ winding, L_{self} and L_m represent the self- and the mutual-inductance of the $a1$ winding and e_{a1} represents the back-emf voltage of the $a1$ winding due to the permanent magnet.

Neglecting leakage currents caused by the common mode voltages, the sum of each 3-phase current is zero because of the Y-connected winding structure. Thus, the voltage equation of a1 phase can be simplified as shown in (2).

$$v_{a1} = R_s i_{a1} + \left(L_{self} - L_m\right)\frac{di_{a1}}{dt} + e_{a1} \quad (2)$$

Replacing $L_{self} - L_m$ by L_s what is called a synchronous inductance, the voltage equation of set 1 becomes the same as that of a conventional 3-phase surface mounted PM motor. Then, the voltage equation of set 1 in a d-q stationary frame can be described by (3).

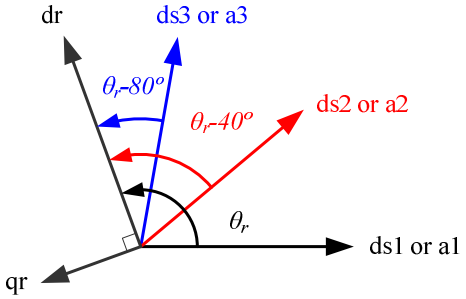

Fig. 4. The relation between rotor and stator frame.

$$v_{ds1}^s = R_s i_{ds1}^s + L_s\frac{di_{ds1}^s}{dt} + e_{ds1}^s$$
$$v_{qs1}^s = R_s i_{qs1}^s + L_s\frac{di_{qs1}^s}{dt} + e_{qs1}^s \quad (3)$$

Assuming the back-emf induced by the permanent magnet as a sinusoidal wave, the voltage equation of set 1 in a d-q rotor reference frame is given by (4).

$$v_{ds1}^r = R_s i_{ds1}^r + L_s\frac{di_{ds1}^r}{dt} - \omega_r L_s i_{qs1}^r$$
$$v_{qs1}^r = R_s i_{qs1}^r + L_s\frac{di_{qs1}^r}{dt} + \omega_r\left(L_s i_{ds1}^r + \lambda_f\right) \quad (4)$$

where λ_f is the flux linkage between the stator windings and the permanent magnet and ω_r is the electrical angular velocity of the rotor.

Similarly, the transformation for the other sets can be derived and they are illustrated by (5) and (6).

$$v_{ds2}^r = R_s i_{ds2}^r + L_s\frac{di_{ds2}^r}{dt} - \omega_r L_s i_{qs2}^r$$
$$v_{qs2}^r = R_s i_{qs2}^r + L_s\frac{di_{qs2}^r}{dt} + \omega_r\left(L_s i_{ds2}^r + \lambda_f\right) \quad (5)$$

$$v_{ds3}^r = R_s i_{d3}^r + L_s\frac{di_{ds3}^r}{dt} - \omega_r L_s i_{qs3}^r$$
$$v_{qs3}^r = R_s i_{qs3}^r + L_s\frac{di_{qs3}^r}{dt} + \omega_r\left(L_s i_{ds3}^r + \lambda_f\right) \quad (6)$$

The relation between each rotor and stator-axis used for the frame transformation is shown in Fig. 4. The axis ds1 and dr represent the stator d-axis of the set 1 and the rotor d-axis. Using this relation, all variables are written in the same reference frame.

In the surface mounted PM motor, the current which contributes to the torque generation is only the rotor q-axis component. Thus, the torque generated by the set 1 can be described as (7).

$$T_{e1} = \frac{3}{2}\frac{P}{2}\lambda_f i_{qs1}^r \quad (7)$$

where P represents the number of pole. There are three independent winding sets and thus the total torque is the sum of the torque generated by the three sets. As a consequence, the total toque generated by the 9-phase motor can be expressed as (8).

$$T_e = \frac{3}{2}\frac{P}{2}\lambda_f\left(i_{qs1}^r + i_{qs2}^r + i_{qs3}^r\right) \quad (8)$$

B. Control Strategy

The control scheme for the proposed 9-phase motor drive system is shown in Fig. 5. It is a cascaded structure made up of one speed controller and three current controllers. The speed controller generates the torque reference to track the speed reference. And the torque reference is converted to the current reference according to (8). In normal operation, the current reference of each inverter set is kept as the same value like (9).

$$i_{qs1}^{r*} = i_{qs2}^{r*} = i_{qs3}^{r*} = \frac{T_e^*}{3\left(\frac{3}{2}\frac{P}{2}\lambda_f\right)} \quad (9)$$

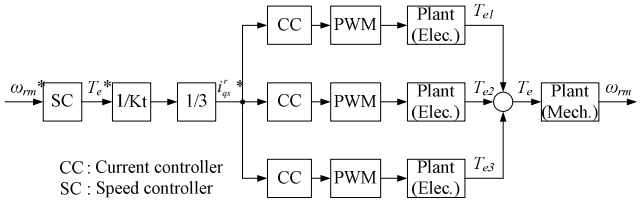

Fig. 5. Control scheme for the 9-phase motor drive system.

There are three sets of 3-phase current controllers to drive the 9-phase motor. Because there is no electrical inter-connection among three sets, each set of windings can be individually controlled. Also, the voltage equation of each set is the same as that of a conventional 3-phase motor. Thus, a well-known synchronous frame PI current controller with feed forward back emf compensation term can be applied. The transfer function of the set 1 from the current error to the controller output voltage can be given by (10).

$$V_{dqs1}^{r*} = \left(K_p + \frac{K_i}{s}\right)\left(I_{dqs1}^{r*} - I_{dqs1}^{r}\right) + V_{dqs1\_ff}^{r} \tag{10}$$

where K_p and K_i are the proportional and integral gain respectively, and the feed forwarding term in (10), can be expressed as (11).

$$\begin{aligned} V_{ds1\_ff}^{r} &= -\omega_r L_s I_{qs1}^{r} \\ V_{qs1\_ff}^{r} &= \omega_r \left(L_s I_{ds1}^{r} + \lambda_f\right) \end{aligned} \tag{11}$$

By using this current controller, the steady state errors in the fundamental component of the phase currents are eliminated. However, the phase currents even in the steady state contain several low order harmonic components because the back-emf waveform of the proposed motor is not pure sinusoidal. In addition, there may be the output voltage distortion caused by non-linearity of the inverter. Nevertheless, it is expected that the distortion in the torque given by (8) is reduced considerably. It is because that the current distortion of one set is canceled by the current distortion of the other two sets. That is, the proposed current control method based on the appropriate mathematical modeling of the proposed motor makes it possible that the torque distortion can be reduced remarkably with the easy and simple torque control method.

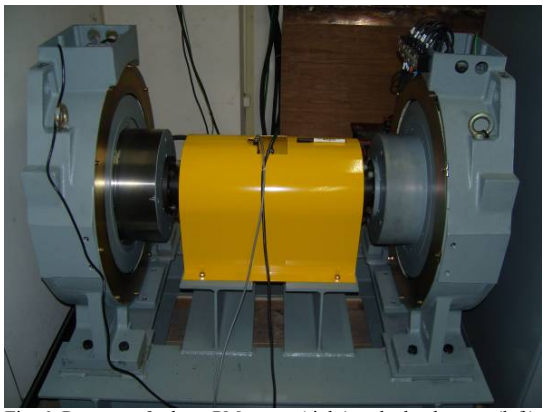
Fig. 6. Prototype 9-phase PM motor (right) and a load motor (left).

TABLE II
PARAMETERS OF THE PROTOTYPE MOTOR

Rated Power	15 kW
Rated Speed	191 r/min
Rated Torque	720 Nm
Pole / Slot	32 / 36
Phase Resistance	0.57 mΩ
Phase Inductance	23 mH
Permanent Magnet Flux Linkage	0.7 Wb

IV. EXPERIMENTAL RESULTS

To evaluate the validity of the proposed system, a small scaled prototype motor and its drive system have been developed. The 15kW 9-phase prototype PM motor is shown in Fig. 6. The left one in Fig. 4 is the 3-phase load motor and the right one is the 9-phase prototype motor. The parameters of the prototype motor are listed in Table II.

To confirm the back-emf shape of the prototype motor, it has been operated at a constant speed of 120 r/min (32 Hz). The a-phase back-emf waveforms of the set 1 and the set 2 are shown in Fig. 7. The magnitude of the fundamental component is about 150 V and the 3rd and 5th harmonics are about 4% and 2% of the fundamental component respectively as shown in their FFT results. The line-to-line voltages between a- and b-phases of the two sets are shown in Fig. 8. The 3rd harmonics are canceled out in the line-to-line voltage.

The phase currents controlled by (10) and (11) are shown in Fig. 9. The bandwidth of the current controller is set to 200 Hz and that of the speed controller is set to 2 Hz. The speed has been controlled by the prototype motor to a constant speed of 120 r/min and the load torque has been set to 630 Nm. It takes the form of almost pure sinusoidal except small amount of the 5th order harmonic distortion which is 1.2% of the fundamental one. The phase difference between each set is 40º in electrical angle.

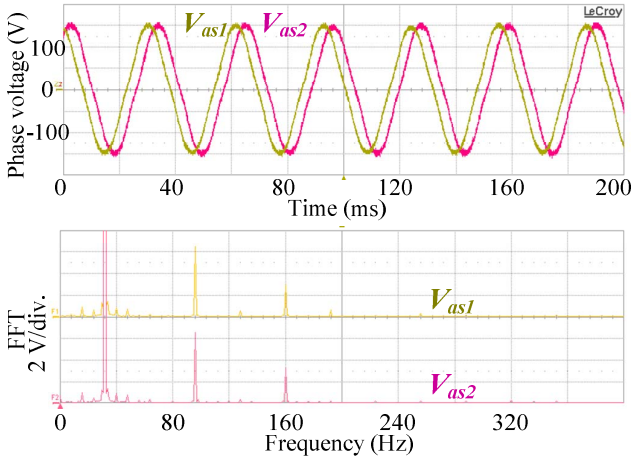

Fig. 7. Phase voltage waveforms (Top: a-phase voltage of set 1 and set 2, bottom: FFT result of the phase voltage).

The *q*-axis current waveforms of the three sets are shown in Fig 10 of which the operating condition is the same with Fig. 9. The average value of the magnitude of each current is about 12 A and the ripple current is less than 0.3 A. The ripple current contains somewhat low frequency components as well as the 6th order ones of the synchronous frequency. As expected, in the sum of three q-axis currents, the 6th order harmonic component caused by non-ideal back-emf waveform as well as the inverter nonlinearity has been reduced remarkably due to the symmetry of the current control system.

The magnitude of the 2nd and 3rd order harmonic components in the q-axis currents is similar to the each q-axis current which seems there is no reduction. However, the magnitude of the fundamental frequency in the q-axis currents summation is three times larger than each q-axis current of three sets. Thus, the ratio between the harmonic distortion and the fundamental current is reduces to one third of the ratio of each set. As a consequence, it can be said that the torque distortion caused by the electrical drive system has been reduced conspicuously by the proposed 9-phase current control system.

Fig. 11 shows the experimental result of the operation under a fault condition where the set 3 is separated from the system. Therefore, the current of the set 3 is zero and the load torque is reduced to 420 Nm which is two third of the load torque in Fig. 10. In this case the 6th order harmonics are not cancelled well because only two sets are operating. But, still the ratio between 6th order and fundamental one is reduced to a half due to interleaved operation of two sets.

V. CONCLUSIONS

This paper proposes the 9-phase PM motor and its drive system for the ultra high-speed elevator. The mathematical model of the 9-phase PM motor has been evaluated based on its inherent structure. Using the simplified mathematical model, the proposed 9-phase motor can be controlled by the conventional 3-phase current control algorithm. Even though, the distortion of each 3-phase current is inevitable because of the non-ideal back-emf, the distortion on the total driven torque of the motor can be reduced conspicuously due to the symmetry of the current controller. The validity of the proposed mathematical modeling and the control system of the prototype 9-phase motor has been verified by experimental results.

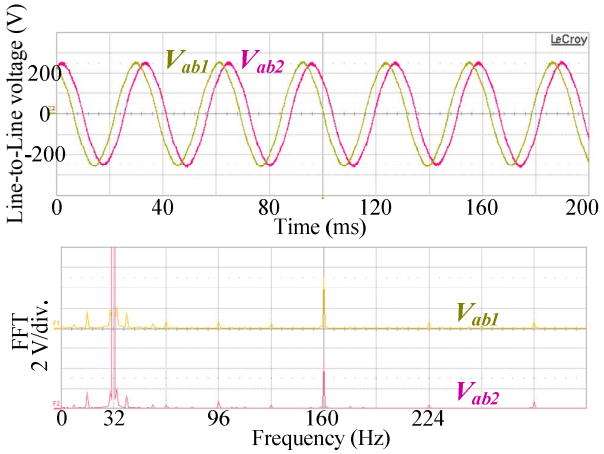

Fig. 8. Line-to-line voltage waveforms (Top: Vab of set 1 and set 2, bottom: FFT result of the line-to-line voltage).

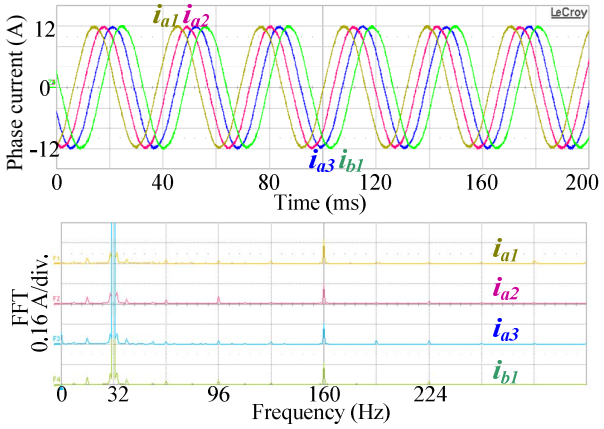

Fig. 9. Phase current waveforms (Top: a-phase currents of three sets and b-phase current of set 1, bottom: FFT result of phase currents).

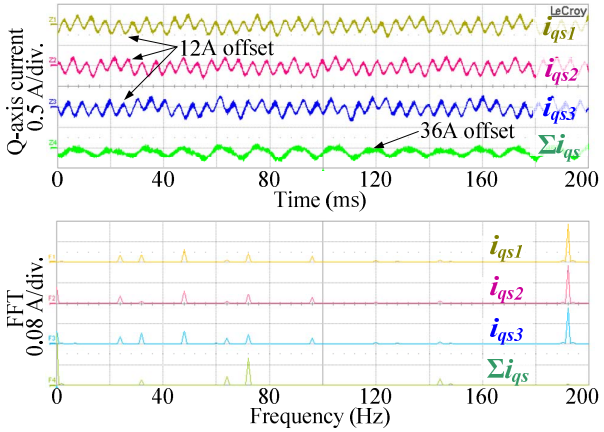

Fig. 10. Q-axis currents in a normal operation (Top: q-axis currents of three sets, bottom: FFT result of the q-axis currents).

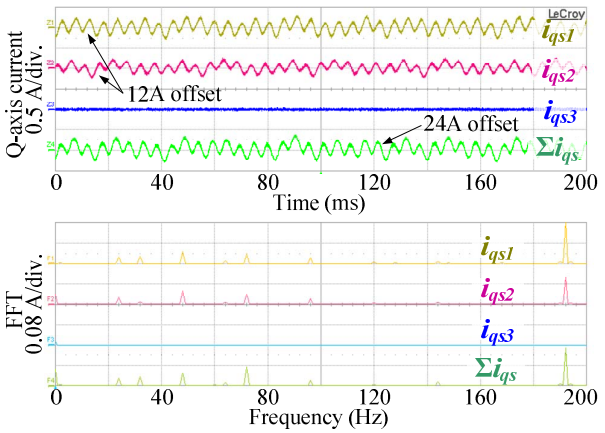

Fig. 11. Q-axis currents in a fault condition (Top: q-axis currents of three sets, bottom: FFT result of the q-axis currents).

REFERENCES

[1] M. A. Abbas, R. Christen, and T. M. Jahns, "Six-phase voltage source inverter driven induction motor," *IEEE Trans. Industry Applications*, vol. IA-20, no. 5, pp. 1251-1259, Sep./Oct. 1984.

[2] R. Kianinezhad, B. Nahid-Mobarakeh, L. Baghli, F. Betin, and G. A. Capolino, "Modeling and control of six-phase symmetrical induction motor under fault condition due to open phases," *IEEE Trans. Industrial Electronics*, vol. 55, no. 5, pp. 1966-1977, May 2008.

[3] M. A. Shamsi-Nejad, B. Nahid-Mobarakeh, S. Pierfederici, and F. Meibody-Tabar, "Fault tolerant and minimum loss control of double-star synchronous motors under open phase conditions," IEEE Trans. Industrial Electronics, vol. 55, no. 5, pp. 1956-1965, May 2008.

[4] N. Toshiaki, K. Hideya, S. Youichi, and N. Shigeo, "World's fastest elevator (1,010 m/min)," Toshiba review, vol.57, no. 6, pp. 58-63, 2002.

[5] J.R. Hendershot Jr. and TJE Miller, *Design of brushless permanent-magnet motors*, Magna Physics-Oxford, 1994.

[6] Dae-Woong Chung, Hyung-Min Ryu,Young-Min Lee, Lo-Won Kang, Seung-Ki Sul, Seok-Joo Kang, Jun-Ho Song, Joong-Seok Yoon, Kil-Haeng Lee, and Jong-Ho Suh, "Drive systems for high-speed gearless elevators," *IEEE Industry Applications Magazine*, vol. 7, no. 5, pp. 52-56, Sep./Oct. 2001.